

Pressure-induced transition from a spin glass to an itinerant ferromagnet in the half-doped manganite $L_{0.5}\text{Ba}_{0.5}\text{MnO}_3$ ($L = \text{Sm}$ and Nd) with quenched disorder

N. Takeshita,^{1,*} C. Terakura,¹ D. Akahoshi,¹ Y. Tokura,^{1,2} and H. Takagi^{1,3,4}

¹*Correlated Electron Research Center (CERC), National Institute of Advanced Industrial Science and Technology (AIST), Tsukuba, Ibaraki 305-8562, Japan*

²*Department of Applied Physics, University of Tokyo, 7-3-1 Hongo, Bunkyo-ku, Tokyo 113-8656, Japan*

³*Department of Advanced Materials Science, University of Tokyo, 5-1-5 Kashiwa-no-ha, Kashiwa 277-8581, Japan*

⁴*CREST, Japan Science and Technology Corporation (JST)*

(Received 9 February 2004; published 21 May 2004)

The effect of quenched disorder on the multiphase competition has been investigated by examining the pressure phase diagram of the half-doped manganite $L_{0.5}\text{Ba}_{0.5}\text{MnO}_3$ ($L = \text{Sm}$ and Nd) with A-site disorders. $\text{Sm}_{0.5}\text{Ba}_{0.5}\text{MnO}_3$, a spin-glass insulator at ambient pressure, switches to a ferromagnetic metal through an intermediate state with increasing pressure, followed by a rapid increase of the ferromagnetic transition temperature T_C . The rapid increase of T_C was also confirmed for $\text{Nd}_{0.5}\text{Ba}_{0.5}\text{MnO}_3$. These observations indicate that the unusual suppression of the multicritical phase boundary in the A-site disordered system, previously observed as a function of the averaged A-site ionic radius, is essentially controlled by the pressure and hence the bandwidth. The effect of quenched disorder is therefore much more enhanced with approaching the multicritical region.

DOI: 10.1103/PhysRevB.69.180405

PACS number(s): 75.30.Kz, 71.30.+h

One of the hallmarks of strongly correlated electron physics is the multiphase competition produced by a delicate interplay among charge, spin, and orbital degrees of freedom.^{1,2} An appealing example of such multicriticality can be seen in perovskite manganites. Competing interactions/orders inherent in the manganites, such as double-exchange ferromagnetism versus superexchange antiferromagnetism and charge-orbital order versus metallic state, tend to produce the multicritical state where external stimuli occasionally cause the dramatic phase conversion, e.g., between a metal and an insulator, or between a ferromagnet and an antiferromagnet.³ The colossal magnetoresistance (CMR) phenomena⁴ are believed to be a consequence of such phase competitions.

Recently, the vital role of quenched disorder in the critical region of manganites has been attracting considerable interest. The quenched disorder⁵ may result in a phase separation⁶ into the competing two ordered phases on various time and length scales, which substantially modifies the criticality and hence the response to the external field. The first suggestion came from the observation of relaxorlike behavior induced by Cr doping on the Mn sites in the charge/orbital ordered (CO/OO) state.^{7,8} This is highly likely associated with the ferromagnetic (FM) metallic clusters coexisting with the background CO/OO state. The effect of quenched disorder on the A site was subsequently examined, which shows a drastic modification of the phase diagram as a function of the average A-site ionic radius.

The half-doped manganites $L_{0.5}\text{Ba}_{0.5}\text{MnO}_3$ ($L = \text{Lanthanides}$) are one of the ideal systems to explore the physics of quenched disorder. The perovskite manganites in this chemical composition have two possible forms of the crystal structure, depending on the synthetic condition.⁹ One is with the A sites randomly occupied by L^{3+} and Ba^{2+} ions. The melt-quenched sample shows the complete solid solu-

tion of L and Ba ions on the A sites with a simple cubic structure as the average structure. The other is the A-site ordered perovskite with the alternate stack of LO and BaO sheets along the c axis with intervening MnO_2 sheets. This is due to the large difference in the ionic radii of L^{3+} and Ba^{2+} . The respective MnO_2 sheets in this tetragonal form are free from random potential which would otherwise arise from the Coulomb potential or local strain from the random occupation of L/Ba on the A sites.

The phase diagram^{10,11} of ordered $L_{1/2}\text{Ba}_{1/2}\text{MnO}_3$ as a function of ionic radius is schematically shown by the dotted line in Fig. 1. The increase of ionic radius results in the reduction of Mn-O bond bending and hence the increases of the bandwidth. With relatively small L ions from Dy to Sm, the charge exchange (CE)-type charge-ordered state with diagonal orbital stripes develops at low temperatures. With larger L ions from Nd to La, on the other hand, the ferromagnetic metal phase and, eventually, the A-type antiferromagnetic phase with ordering of $d_{x^2-y^2}$ orbitals are stabilized upon cooling the sample. These phases meet with each other at around $L = \text{Nd}$, forming a well-defined multicritical point. When the solid solution of L^{3+} and Ba^{2+} is formed, however, this multicritical region is drastically altered.¹¹ The solid line in Fig. 1 indicates the phase diagram of A-site disordered $L_{0.5}\text{Ba}_{0.5}\text{MnO}_3$. It is clear that the phase transitions near the multicritical point are suppressed significantly. In contrast to the ordered $L_{0.5}\text{Ba}_{0.5}\text{MnO}_3$, the charge- and orbital-ordered phase goes away and alternatively a spin glass phase without long-range order in any charge and orbital sectors emerges. With increasing the ionic radius, the ferromagnetic metal phase takes over the spin-glass phase at around Nd. On this way, an intermediate phase is observed.¹¹ This phase is assumed to be a microscopic phase-separated state. The A-type antiferromagnetic phase, however, does not show up at low temperatures. Besides, as compared with the

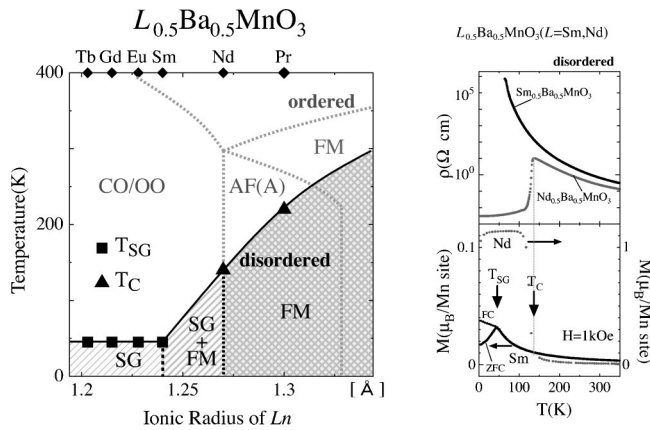


FIG. 1. Phase diagrams as a function of ionic radius of L ions are shown in the left-hand side panel for A-site ordered and disordered $L_{0.5}\text{Ba}_{0.5}\text{MnO}_3$. (Data taken from Ref. 11 by Akahoshi *et al.*) The solid and dotted lines indicate those for disordered and ordered systems, respectively. FM, AF, SG, and CO/OO denote ferromagnetic metal, antiferromagnet, spin glass, and charge and orbital ordered state, respectively. The right-hand side panel indicates the temperature-dependent resistivity and magnetization for A-site disordered $\text{Sm}_{0.5}\text{Ba}_{0.5}\text{MnO}_3$ and $\text{Nd}_{0.5}\text{Ba}_{0.5}\text{MnO}_3$.

A-site ordered systems, the ferromagnetic phase extends to the smaller ionic radius and the ferromagnetic transition temperature, T_C , is appreciably suppressed near the critical region.

The contrast between the A-site ordered and the disordered systems demonstrates a substantial influence of quenched disorder on the multiphase competition in the manganites. However, it should be emphasized here that the control parameter of the disordered system is not only the bandwidth, but also the degree of disorder. By changing the L ion, the degree of disorder is inherently modified associated with the change in the ionic radius. It is difficult to identify which factor plays a dominant role in the unusual phase diagram of the disordered system. For example, the rapid decrease of T_C in the ferromagnetic phase with approaching the critical region can be interpreted as an *enhanced* influence of quenched disorder in the critical region. Alternately, it may be understood in terms of the increased disorder with decreasing the ionic radius of L ions from those comparable with large Ba ions.

To separate the two contributions arising from the disorder and the bandwidth, we have employed hydrostatic pressure to modify the bandwidth alone, while keeping the degree of disorder constant. We have selected two A-site disordered compounds, $\text{Sm}_{0.5}\text{Ba}_{0.5}\text{MnO}_3$ and $\text{Nd}_{0.5}\text{Ba}_{0.5}\text{MnO}_3$, and applied hydrostatic pressures up to 10 GPa. We found a pressure induced spin glass insulator to ferromagnetic metal transition, which can be mapped onto the phase diagram obtained by examining the solid-solution effect. This clearly demonstrates that the unusual phase diagram of disordered $L_{0.5}\text{Ba}_{0.5}\text{MnO}_3$ arises from the bandwidth.

The A-site solid solutions of $L_{0.5}\text{Ba}_{0.5}\text{MnO}_3$ ($L = \text{Sm}$ and Nd) were grown by the floating-zone method in a single

crystalline form. The starting polycrystalline rods were prepared by a standard solid-state reaction. The x-ray powder diffraction patterns of the resultant crystalline rods indicate the formation of single phase $L_{0.5}\text{Ba}_{0.5}\text{MnO}_3$ without any evidence for the A-site ordering. The resistivity and magnetization data of disordered $\text{Sm}_{0.5}\text{Ba}_{0.5}\text{MnO}_3$ and $\text{Nd}_{0.5}\text{Ba}_{0.5}\text{MnO}_3$, at ambient pressure, are shown in the right-hand side panel of Fig. 1. The resistivity of disordered $\text{Sm}_{0.5}\text{Ba}_{0.5}\text{MnO}_3$ shows an insulating behavior down to the lowest temperature measured, and no evidence for the long-range charge ordering is observed. Corresponding to the phase line T_{SG} in Fig. 1, we observe a spin glass transition at 50 K in the magnetization, but no appreciable anomaly at T_{SG} is observed in the resistivity. In the $\text{Nd}_{0.5}\text{Ba}_{0.5}\text{MnO}_3$ sample, the resistivity shows a very rapid decrease below 140 K, which corresponds to the transition to a ferromagnetic metal phase. Note that the Curie temperature here is reduced to almost a half of the cation ordered $\text{Nd}_{1/2}\text{Ba}_{1/2}\text{MnO}_3$.^{10,11} Hydrostatic pressures up to 10 GPa were applied to those two crystals by a cubic-anvil-type pressure apparatus.¹² The electrical resistivity and the ac susceptibility measurements were conducted within the pressure cell down to $T = 4.2$ K.

The results of resistivity measurements on $\text{Sm}_{0.5}\text{Ba}_{0.5}\text{MnO}_3$ under various pressures were summarized in the left-hand side panel of Fig. 2. Up to 6 GPa, no appreciable change was observed in the electrical resistivity measurements, except for the decrease of the magnitude of resistivity. The resistivity shows an insulating behavior down to 4.2 K, suggesting that the system remains in the spin glass phase. These results strongly suggest that the spin glass phase exists below 4 GPa. Above 4 GPa, in contrast, a substantial change was observed at low temperatures. The resistivity shows a rapid decrease upon cooling, which is a characteristic behavior of the transition to a ferromagnetic metal. The spin glass-ferromagnet transition is observed also by ac susceptibility χ_{AC} measurements shown also in the left-hand side panel of Fig. 2. At low pressures, we clearly observe a kink around 50 K, which represents the spin glass transition. Above 8 GPa, a drastic change of the χ_{AC} is observed, which very likely indicates the appearance of ferromagnetic transition. This switching from spin glass to ferromagnet occurs at higher pressure than the appearance of metallic behavior in the resistivity. It appears to imply the presence of a two phase mixture around the phase boundary. Indeed, even though the resistivity shows metallic behaviors, the residual resistivities between 6 and 10 GPa are higher than the Ioffe-Regal limit, which can be naturally understood by the two phase picture. These behaviors can be visually summarized as a phase diagram in Fig. 3. We immediately notice that the phase changes as a function of pressure are essentially the reproduction of those with the average ionic radius on the A site.

It is now clear that the dominant controlling factor of the unusual phase diagram in disordered $L_{0.5}\text{Ba}_{0.5}\text{MnO}_3$ is the bandwidth. Then, the pressure dependence of transition temperatures in disordered $\text{Nd}_{0.5}\text{Ba}_{0.5}\text{MnO}_3$ should be connected to that of $\text{Sm}_{0.5}\text{Ba}_{0.5}\text{MnO}_3$ by shifting the pressure axis. The right-hand side panel of Fig. 2 indicates the evolution of the

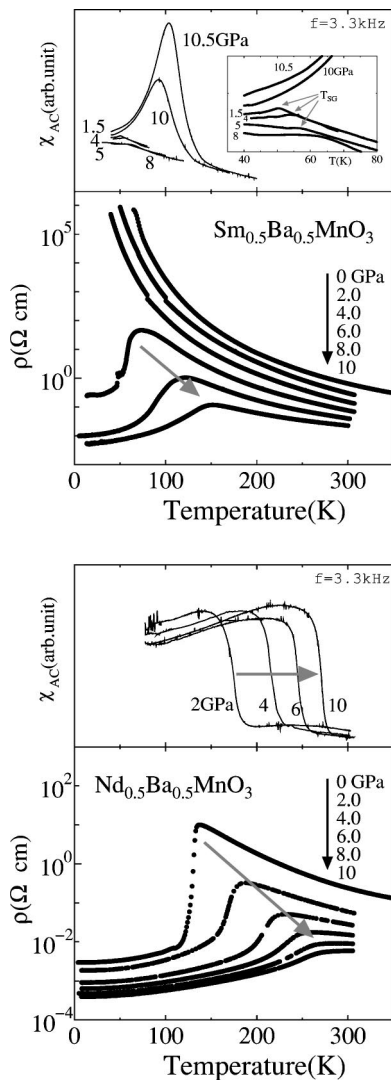


FIG. 2. Temperature-dependent resistivities and ac susceptibilities in the same sample under various pressures for A-site disordered $\text{Sm}_{0.5}\text{Ba}_{0.5}\text{MnO}_3$ (left-hand side) and $\text{Nd}_{0.5}\text{Ba}_{0.5}\text{MnO}_3$ (right-hand side).

temperature dependent resistivity and the ac susceptibility with increasing pressure for the A-site disordered $\text{Nd}_{0.5}\text{Ba}_{0.5}\text{MnO}_3$. T_C defined as a temperature of resistivity anomaly shows a rapid increase with increasing pressure. At high pressures, the resistivity anomaly tends to become weaker, which makes the determination of T_C ambiguous. In the ac susceptibility, however, well defined anomalies associated with the ferromagnetic transition (indicated by arrows) were still observable, which provide us with a more reliable estimate of T_C . Thus, obtained pressure dependence of T_C is plotted in Fig. 3. By shifting by 10 GPa, the T_C - P curve of disordered $\text{Nd}_{0.5}\text{Ba}_{0.5}\text{MnO}_3$ seems to be smoothly connected to that of $\text{Sm}_{0.5}\text{Ba}_{0.5}\text{MnO}_3$. This provides further evidence for the dominance of pressure as the controlling parameter.

Another important point is that T_C of $\text{Nd}_{0.5}\text{Ba}_{0.5}\text{MnO}_3$ tends to saturate with increasing pressure. In the saturation region, T_C recovers to almost 300 K, which is close to those

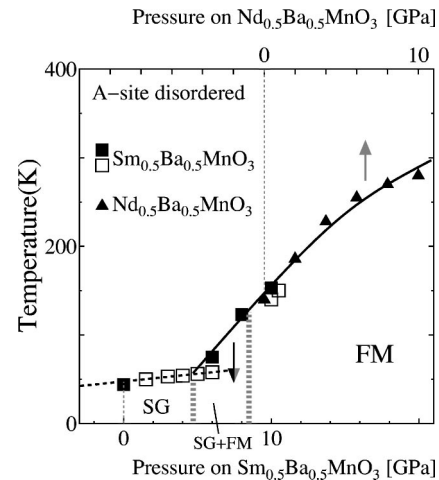


FIG. 3. Pressure phase diagram of A-site disordered $\text{Sm}_{0.5}\text{Ba}_{0.5}\text{MnO}_3$ and $\text{Nd}_{0.5}\text{Ba}_{0.5}\text{MnO}_3$ determined from the resistivity (filled square and triangle) and the magnetic susceptibility (open square) data shown in Fig. 2. The pressure axis for $\text{Nd}_{0.5}\text{Ba}_{0.5}\text{MnO}_3$ is shifted by 10 GPa.

observed for ordered $L_{1/2}\text{Ba}_{1/2}\text{MnO}_3$ with $L=\text{Nd}$ and Pr . These observations strongly suggest that the suppression of T_C is much reduced once removed from the critical region. Note again that the degree of disorder is kept constant in this experiment. We therefore conclude that the effect of quenched disorder is substantially *enhanced* when coupled with the (multi)criticality.

Recently, it was pointed out that the quenched disorder triggers a phase separation into ferromagnetic and charge-ordered domains.¹³ In this scenario, the formation of a clustered state with randomly oriented ferromagnetic clusters results in the decreases of the clean limit T_C to a much lower T_C in the ferromagnetic region. This accounts for the anomalous suppression of T_C with approaching the critical region.¹⁴ More recent works claim that the state below the clean limit T_C is not statically clustered, is a homogeneous state with substantial critical charge/lattice fluctuations induced by quenched disorder.¹⁵ Present pressure measurement alone cannot specify whether the phase separation is static or dynamic.

In summary, we have observed a pressure-induced switching of a spin glass into a ferromagnet in a half-doped manganese $\text{Sm}_{0.5}\text{Ba}_{0.5}\text{MnO}_3$ with quenched disorder, which is followed by a rapid increase of Curie temperature upon pressure. The remarkably rapid increase of Curie temperature was confirmed also in itinerant ferromagnet $\text{Nd}_{0.5}\text{Ba}_{0.5}\text{MnO}_3$ with a slightly larger ionic radius. Thus, obtained pressure phase diagram can be mapped onto the unusual phase diagram of disordered $L_{0.5}\text{Ba}_{0.5}\text{MnO}_3$ as a function of ionic radius, indicating that the critical control parameter is the bandwidth under the presence of quenched disorder. It is now firmly established that the effect of quenched disorder is much more enhanced in the critical region, resulting in a stronger suppression of phase transition with approaching the multicritical point. The high pressure measurements have proved themselves as a remarkably useful probe to explore

the physics of quenched disorder in multiphase competing systems.

The authors would like to thank Y. Motome, N. Nagaosa, and Y. Tomioka for their enlightening discussion. This

work is partly supported by a Grant-in-Aid for Scientific Research from the Ministry of Education, Culture, Sports, Science and Technology, Japan, and the New Energy and Industrial Technology Development Organization (NEDO), Japan.

*Electronic address: takeshita.n@aist.go.jp

¹Y. Tokura and N. Nagaosa, *Science* **288**, 462 (2000).

²E. Dagotto, T. Hotta, and A. Moreo, *Phys. Rep.* **344**, 1 (2001).

³Y. Tomioka and Y. Tokura, *Phys. Rev. B* **66**, 104416 (2002).

⁴H. Kuwahara, Y. Tomioka, A. Asamitsu, Y. Moritomo, and Y. Tokura, *Science* **270**, 961 (1995).

⁵R.B. Griffiths, *Phys. Rev. Lett.* **23**, 17 (1969).

⁶M. Uehara, S. Mori, C.H. Chen, and S.-W. Cheong, *Nature (London)* **399**, 560 (1999).

⁷B. Raveau, A. Maignan, and C. Martin, *J. Solid State Chem.* **130**, 162 (1997).

⁸T. Kimura, Y. Tomioka, R. Kumai, Y. Okimoto, and Y. Tokura, *Phys. Rev. Lett.* **83**, 3940 (1999).

⁹F. Millange, V. Caignaert, B. Domenges, and B. Raveau, *Chem.*

Mater. **10**, 1974 (1998).

¹⁰T. Nakajima, H. Kageyama, H. Yoshizawa, and Y. Ueda, *J. Phys. Soc. Jpn.* **71**, 2843 (2002).

¹¹D. Akaoshi, M. Uchida, Y. Tomioka, T. Arima, Y. Matsui, and Y. Tokura, *Phys. Rev. Lett.* **90**, 177203 (2003).

¹²N. Mōri, Y. Okayama, H. Takahashi, Y. Haga, and T. Suzuki, *Jpn. J. Appl. Phys.* **8**, 182 (1993).

¹³J. Burgy, M. Mayr, V. Martin-Mayor, A. Moreo, and E. Dagotto, *Phys. Rev. Lett.* **87**, 277202 (2001).

¹⁴H. Aliaga, D. Magnoux, A. Moreo, D. Poilblanc, S. Yunoki, and E. Dagotto, *Phys. Rev. B* **68**, 104405 (2003).

¹⁵Y. Motome, N. Furukawa, and N. Nagaosa, *Phys. Rev. Lett.* **91**, 167204 (2003).